Microchimica Acta (2022) 189: 252
https://doi.org/10.1007/s00604-022-05316-3

REVIEW ARTICLE

Label-free electrochemical microfluidic biosensors: futuristic point-of-care analytical devices for monitoring diseases

Ghasem Ebrahimi[1,2] · Parvin Samadi Pakchin[1] · Amir Shamloo[3] · Ali Mota[2] · Miguel de la Guardia[4] · Hossein Omidian[5] · Yadollah Omidi[5]

Received: 3 March 2022 / Accepted: 20 April 2022 / Published online: 10 June 2022
© The Author(s), under exclusive licence to Springer-Verlag GmbH Austria, part of Springer Nature 2022

Abstract

The integration of microfluidics with electrochemical analysis has resulted in the development of single miniaturized detection systems, which allows the precise control of sample volume with multianalyte detection capability in a cost- and time-effective manner. Microfluidic electrochemical sensing devices (MESDs) can potentially serve as precise sensing and monitoring systems for the detection of molecular markers in various detrimental diseases. MESDs offer several advantages, including (i) automated sample preparation and detection, (ii) low sample and reagent requirement, (iii) detection of multi-analyte in a single run, (iv) multiplex analysis in a single integrated device, and (v) portability with simplicity in application and disposability. Label-free MESDs can serve an affordable real-time detection with a simple analysis in a short processing time, providing point-of-care diagnosis/detection possibilities in precision medicine, and environmental analysis. In the current review, we elaborate on label-free microfluidic biosensors, provide comprehensive insights into electrochemical detection techniques, and discuss the principles of label-free microfluidic-based sensing approaches.

Keywords Biosensor · Electrochemical detection · Label-free sensing · Microfluidics · Point-of-care

Introduction

Microfluidic technology allows the processing of trivial amounts of fluids (10^{-9} to 10^{-18} L) in microchannels and chambers through a laminar flow [1]. Technically, a microfluidic chip consists of an inlet, channel, mixer, valve, and outlet (or signal detector). Various inorganic materials (e.g., glass, silica, ceramics), polymers (e.g., elastomers, thermoplastics, thermosets), and papers are used to manufacture microfluidic chips. Of these, polymers and paper have been extensively studied because of their processability and affordable production. Polymeric organosilicon, polydimethylsiloxane (PDMS), and paper are the most widely used materials for constructing microfluidic-based microdevices [2]. For example, using a highly sensitive paper-based chip anchored with zinc-doped carbon dots, copper ions were quantitatively sensed through fluorescence detection with a low limit of detection (LOD) of 0.018 μg/L [3].

Microfluidic technology allows (i) the separation of different analytes with high resolution, (ii) assisted synthesis and functionalization of monodisperse colloidal systems, and (iii) simultaneous detection of multiple analytes with a fast reaction time at a relatively low cost [4–7]. Additionally, human handling errors and the possibility of false-positive results can be minimized/eliminated with automated microfluidic systems [8]. By integrating the microfluidic systems with a designated sensing modality, a new class of portable detection devices has been developed. Such devices can be used as point-of-care (POC) tools for rapid analysis of biomolecules in resource-limited samples [9].

✉ Yadollah Omidi
yomidi@nova.edu

1 Research Center for Pharmaceutical Nanotechnology, Biomedicine Institute, Tabriz University of Medical Sciences, Tabriz, Iran

2 Department of Biochemistry and Clinical Laboratories, Faculty of Medical Sciences, Tabriz University of Medical Sciences, Tabriz, Iran

3 School of Mechanical Engineering, Sharif University of Technology, Tehran, Iran

4 Department of Analytical Chemistry, University of Valencia, Valencia, Spain

5 Department of Pharmaceutical Sciences, College of Pharmacy, Nova Southeastern University, Fort Lauderdale, FL 33328, USA

An analytical biosensor can quantify the biological response(s) of a bioreceptor through a transducer, which can be used as a diagnostic tool in precision medicine. For specific/selective analysis, various bioreceptors have been used in developing biosensors. These include antibodies (Ab), nanobodies (Nb), aptamers (Ap), molecular-imprinted polymers (MIP), peptides, enzymes, and nucleic acids [10]. Transducers transform biological interaction between the bioreceptor and the analyte into a measurable signal, which can be optical, electrochemical, or mechanical transduction systems. Lastly, the electronic system enhances, processes, and displays the quantified signal(s). The biosensing devices, as suitable POC tools, offer low-cost and fast-response analysis with remarkable LOD values and a wide linear response range [11, 12]. Notably, the integrated microfluidic electrochemical sensing devices (MESDs) can provide label-free detection [13] and real-time analyses of biomolecular events/phenomena [14]. Given the significance of label-free MESDs in quantitative detection/monitoring of molecular markers of diseases, this review provides comprehensive insights into their developments and applications.

Microfluidic technology and materials

Microfluidics is the technology of precise control and manipulation of a small amount of fluid using tens to hundreds of molded/engraved microchannels. Initially, the microfluidic devices were fabricated using silicon and glass, while other materials have gradually been introduced [1]. Microfluidic devices can be fabricated using (i) inorganic materials (e.g., glass, silicon, and ceramic), (ii) thermoplastic polymers and elastomers, as well as (iii) papers. The materials are selected based on cost, production feasibility, detection system, flexibility, electrical conductivity, air permeability, optical transparency, nonspecific adsorption, and resistance to different chemicals [15].

Silicon and glass

Silicon and glass exhibit some specific features, including stable electroosmotic mobility, high thermal conductivity, ease of metal deposition, and compatibility with organic solvents that are routinely utilized in microfluidic devices [16]. However, to fabricate more dynamic components of a microfluidic system, particularly valves and pumps, elastomers are preferred over rigid materials. Unlike glass, silicon is opaque and cannot be used in optical detection methods, as such a hybrid system of a transparent material (glass or polymer) and silicon can be used to overcome this limitation [17]. Neither silicon nor glass possesses all the critical properties (especially permeability to gases) to operate on living cells [18]. In the fabrication of glass and silicon devices, bulk and surface micromachining and buried-channel techniques are employed. The former is the popular technique, in which the microchannels are formed using patterning processes such as wet/dry etching. The channels are then encapsulated by bonding to another wafer via fusion, anodic, and adhesive bonding processes. Some studies have presented a process selection framework for patterning and bonding processes that can favor the microfluidic process flow [19, 20].

Ceramics

Ceramics are inorganic, nonmetallic, and polycrystalline materials with a wide range of attractive functional and structural properties (e.g., high thermal stability, chemical inertness, mechanical strength, and biocompatibility). Ceramic microsystems can easily be constructed without any need for isolated facilities (e.g., clean rooms) and assembled with electronic components such as conductive paths and electrodes that enable the development of integrated devices for electrochemical systems [8, 21]. Due to the ceramic opacity, optical detection in ceramic platforms faces serious challenges. Implementing transparent windows for localized visual and optical analysis and optical fiber integration can be applied to alleviate this issue. Low-temperature cofired ceramic (LTCC) can be utilized to successfully fabricate tightly sealed monolithic ceramic-based microfluidic systems. However, the elevated temperature of the LTCC process is a serious shortcoming that prevents biosensor fabrication using temperature-sensitive entities such as antibodies, enzymes, and the polymeric receptor layer. To overcome this limitation, the biolayer can be deposited on the ceramics' surface following thermal treatment, though many biomaterials are not compatible with this approach.

Polymers

Polymers are the most frequently used materials in manufacturing microchips. They offer some major advantages, including easy access and fabrication, low cost, and amenability to mass production processes such as injection molding and hot embossing [15]. However, the major issue in polymers' microfluidic application is their low Young's modulus of the elasticity, making the polymeric microchannels susceptible to partial deformation and collapse. These materials can be categorized into elastomers, thermoplastics, and thermosets [22]. Characterized as polymers possessing flexible long chains with their glass transition temperature below room temperature, elastomers can be found in almost every industry including healthcare [23]. PDMS is the most popular elastomer used in the development of microfluidic devices. Unlike other hard polymeric materials like polycarbonate (PC) and poly(methyl methacrylate) (PMMA), PDMS provides gas permeation that is crucial for long-term cell culture in sealed microchannels. Its surface contains dominantly nonpolar methyl groups. Thus, the deposition of water-based debris is restricted, which can improve sanitation and clarity, while it might result in difficult bonding with different materials and biomaterials [21]. The resist materials for lithography, especially the photoresist SU-8, are typical examples of the thermoset polymers

used in microfluidic systems. Polyimide, another important material in this class, is a thermally stable and very durable material frequently used in microelectronics [24]. Thermoplastic materials can easily be shaped in a thermal process such as molding, extrusion, and thermoforming. PC, PMMA, poly(vinyl chloride), poly(ethylene terephthalate) (PET), and polystyrene (PS) are the most common thermoplastic materials used in the fabrication of microfluidic devices [24]. Microchambers and microchannels sealed with thermoplastics are not permeable to gas; as such, they are not appropriate for long-term cell studies. For surface modification of thermoplastic materials, the dynamic coating and surface grafting approaches can be utilized.

Paper

Papers exhibit a highly porous structure made of cellulose. In paper-based microfluidic devices, aqueous solutions can accurately be transported by the capillary function through the hydrophilic microchannels restricted by the hydrophobic barriers [25]. The use of paper in the microfabrication of chips offers several advantages, including (i) passive pumping and transferring of fluids in hydrophilic microchannels by the intrinsic capillary potential, (ii) separation of particles from samples (e.g., separation of blood cells), (iii) great possibility for the air permeability, (iv) excellent absorbency with high capacity for the reagents storage due to the large surface-to-volume ratio, and (v) simple fabrication procedure with a great time- and cost-efficiency.

Different methods are used to craft microchannels on paper-based devices. In the cutting method, the channels' boundary is air instead of the hydrophobic barrier. In the patterning procedures, the hydrophilic channels' boundary is formed using hydrophobic materials such as SU-8 photoresist, PDMS, wax, UV-curable ink, indelible ink, PS, hydrophobic silane, acrylic resin, titanium dioxide, alkyl/alkenyl ketene dimer, and polyhydroxybutyrate [26]. The wax printing technique is the most common patterning method, in which a commercially solid-ink printer is applied to the pattern of wax on a paper. The most typical detection method in a paper-based device is the simple visual colorimetry readout that demands minimal equipment, while it is not a quantitative approach. As a cheap material, paper can be used for the mass production of disposable bioassay systems. Depending on the endpoint application, paper can be combined/modified to develop microdevices for specific detection purposes [18].

Label-free electrochemical microfluidic devices

Electrochemical biosensors can technically be constructed by modifying electrode surfaces (e.g., Ag, Au, Pt, carbon, or graphite-based conductors) with biorecognition elements (e.g., Abs, Aps). These analytical methods can quantitatively detect the analyte concentration based on potential or current changes that result in biological interactions at the biomolecule/transducer interface under applied potential or current impulses. In comparison with other calorimetric and optical biosensors, electrochemical biosensors have rapidly been developed due to their high sensitivity, low cost, ease of miniaturization, and simplicity in application. Further, different types of electrochemical labels have commonly been used in some electrochemical biosensors including metal ions, quantum dots, redox agents, redox-active polymers, and enzymes with a detectable product [27–40]. Labels are usually used in sandwich-type biosensors for routine clinical diagnosis such as enzyme-linked immunosorbent assay (ELISA). The label-based biosensors are composed of a bioreceptor, a signal label, and a measurement instrument [41]. The label-free sensing systems present direct data of the bioreceptor-target interaction based on the alteration in the redox probe's interfacial electron-transfer kinetics. As shown in Fig. 1, the $[Fe(CN)_6]^{3-/4-}$ is the most common classical redox couple that is utilized as standard electroactive species in electrochemical measurements [42].

The integration of label-free techniques with microfluidic technologies provides a robust and sound approach for detecting biomolecules, for which electrochemical techniques such as the electrochemical transistor, impedance spectroscopy (EIS), voltammetry, and chronoamperometry can be used (Fig. 2).

Electrochemical transistor

The organic electrochemical transistor (OECT) is an organic thin-film transistor (OTFT) that has extensively been studied.

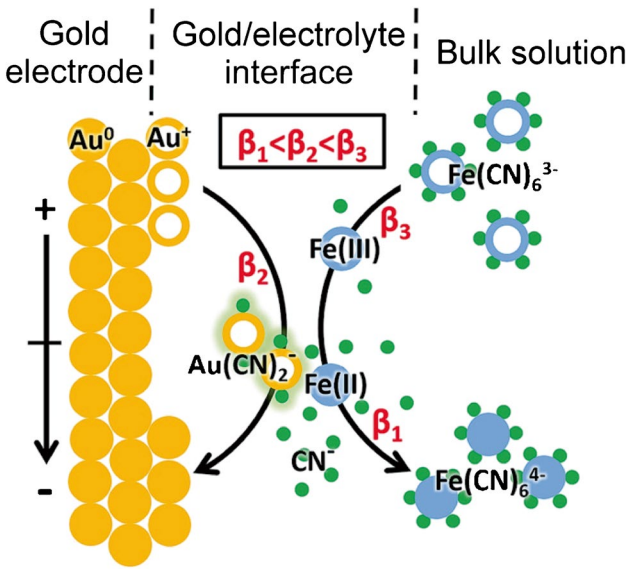

Fig. 1 The suggested mechanism of the interaction between the gold electrode and $[Fe(CN)_6]^{3-/4-}$. ß1, ß2, and ß3 correspond to the cumulative formation constants for $Fe(CN)_6^{4-}$, $Au(CN)_2^-$, and $Fe(CN)_6^{3-}$, respectively. Adapted with permission from [42]

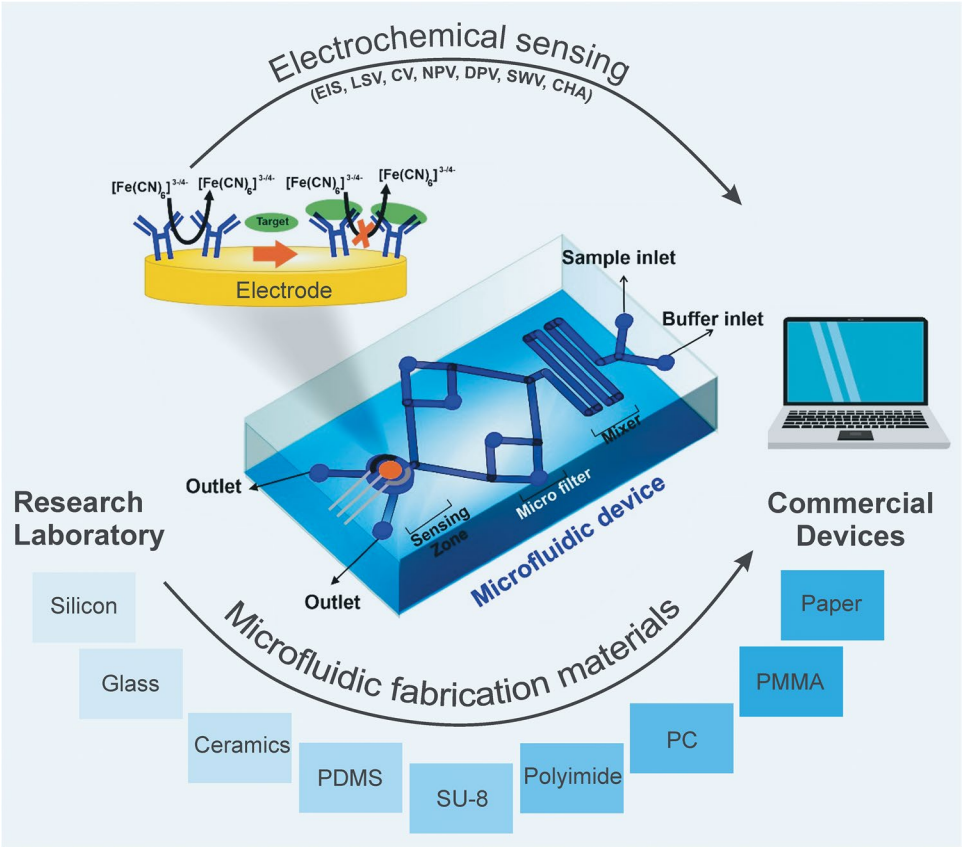

Fig. 2 Schematic representation of electrochemical methods and microfluidic fabrication materials for the design of label-free electrochemical microfluidic devices. PDMS: polydimethylsiloxane, PMMA: poly(methyl methacrylate), PC: polycarbonate, SU-8: bisphenol A Novolac epoxy-based negative photoresist

The OECT offers high sensitivity to chemical and biological analytes, low operation voltage, and high stability in the aqueous environment (Table 1).

OECT can also be readily integrated with microfluidic systems [43, 44]. Lin et al. developed a label-free biosensor to detect an arbitrary DNA oligo-nucleotide using an OECT based on poly(3,4-ethylene dioxythiophene):poly(styrene

Table 1 Selected microfluidic label-free electrochemical transistor

Analytes	Materials	Electroactive species	Electrode type	LOD	Linear range	Sample	Probe	Ref
Glucose	PDMS	H_2O_2	Pt NPs gate electrode	0.1 µM	-	Glucose solutions	GOx	[43]
Arbitrary ssDNA	PDMS	PEDOT:PSS	Au gate electrode	10 pM	-	Solutions	ssDNA	[45]
Glucose lactate cholesterol	PDMS	Ferrocene-PEDOT:PSS	Au planar gate electrode	10 µM (glucose) 50 µM (lactate) 10 µM (cholesterol)	$0.02–1 \times 10^{-3}$ M (glucose) $0.1–2 \times 10^{-3}$ M (lactate) $0.01–0.7 \times 10^{-3}$ M (cholesterol)	Saliva	GOx LOx COx	[44]
miRNA	Silicon	-	SiNW arrays	1 fM	-	Total RNA extracted from Hela cells	PNA	[46]
Glucose	PDMS	H_2O_2 and DHA/AQ	SiNW	-	-	Bacterial media	GOx	[47]

PDMS polydimethylsiloxane, *Pt NPs* platinum nanoparticles, *GOx* glucose oxidase, *PEDOT:PSS* poly(3,4-ethylenedioxythiophene):poly(styrene sulfonic acid), *ssDNA* single-stranded deoxyribonucleic acid, *Lox* lactate oxidase, *Cox* cholesterol oxidase, *miRNA* micro ribonucleic acid, *SiNW* silicon nanowires, *PNA* peptide nucleic acid, *DHA/AQ* active redox system composed of 9,10-dihydroxyanthracene/9,10-anthraquinone

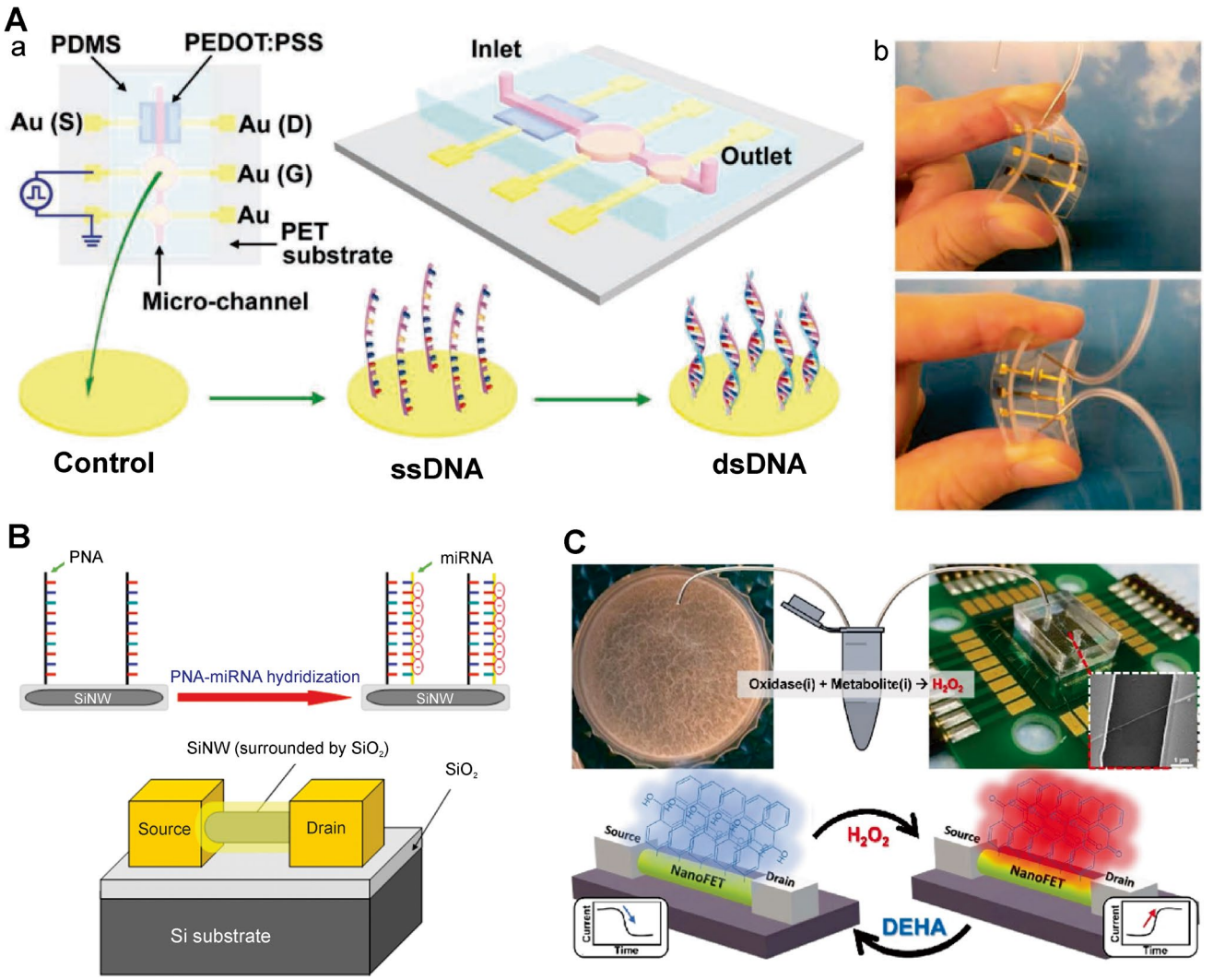

Fig. 3 Integration of microfluidics with an electrochemical transistor for metabolite sensing. (**A**) Organic electrochemical transistors integrated microfluidic system for label-free DNA sensing. (**a**) Schematic diagram of an OECT integrated into a flexible microfluidic system. (**b**) The flexibility of device at both sides. The performance of the device demonstrates a tiny change when the device is bent to both sides. Adapted with permission from [45]. (**B**) Ultrasensitive detection of miRNA via the label-free direct hybridization assay. Adapted with permission from [46]. (**C**) Extracellular bacterial metabolic analysis by silicon-based microfluidic redox-reactive nanoFET biosensor. The biosensor reversely oxidized or reduced in the present H_2O_2 or diethyl hydroxylamine (DEHA), respectively. Adapted with permission from [47]. OECT: organic electrochemical transistor, FET: field-effect transistors

sulfonic acid) (PEDOT:PSS) as the active layer in a flexible microfluidic device [45]. The devices were fabricated on an adaptable PET substrate and integrated with a PDMS-based microfluidic system. The ssDNA probes were immobilized on the surface of the Au gate electrode. The electrochemical signal was created via the hybridization of the ssDNA probes with target DNA. Finally, the resulted current was amplified by the designed platform. The proposed biosensor showed a good target sensitivity at an LOD of 10 pM. As such, this label-free flexible microfluidic DNA sensor was proposed as an overly sensitive, low-cost, and disposable tool to detect the hybridization of DNA at concentrations as low as 1 nM (Fig. 3A). Additionally, a label-free hybridization system for the direct detection of miRNA was applied to facilitate the detection process and eradicate the need for tagging/labeling steps [46]. Peptide nucleic acids (PNA), as bioreceptor, were immobilized on the surface of the *n*-type silicon nanowire (SiNW) array device to enhance the efficiency of hybridization. Thereby, a combination of SiNW field effect-based biosensors and a label-free direct detection methodology was reported to lower the LOD to femtomolar concentrations, which is desirable for the early detection of miRNA in cancer diagnostics (Fig. 3B).

Various approaches have been proposed to monitor the growth of biofilms, assess their susceptibility to drugs, and overcome the emergence of biofilm and infections. For

Table 2 Selected microfluidic label-free electrochemical impedance biosensors

Analytes	Materials	Electroactive species	Electrode type	LOD	Linear range	Sample	Probe	Ref
Testosterone	PDMS-silicon	-	Carbon diamond	0.5 nM	0.5–20 nM	Real sample	MIPs and NIP	[50]
HSA	PMMA	-	Gold	-	100 nM to 5 µM	Solutions and synthetic urine	M13 virus particles (selectively bind to HAS)	[51]
Alprazolam	Paper	MB	Carbon ink	0.025 ng/mL	1–300 ng/mL	Solutions and urine	Electrochemical sensing	[68]
Arbitrary ssDNA	PDMS	Ferrocyanide	Gold	3.8 nM	-	Solutions	ssDNA	[9]
Arbitrary ssDNA	PDMS	Ferrocyanide	Gold	1 nM	-	Solutions	ssDNA	[53]
Methylated DNAs	PDMS	Ferrocyanide	Gold	7.9 pM (GSTP1) 11.8 pM (EFEMP1)	-	Urine	ssDNA	[69]
Cancer cells	PMMA	FeMeOH	Gold	214 captured cells/mm^2	16,400 and $(2.6 \pm 0.0003) \times 10^6$ cancer cells/mL	Cell culture medium	Anti-EpCAM	[54]
PSA and SPON2	PDMS-glass	-	Gold	118 pg/mL (PSA) 238 pg/mL (SPON2)	Adjustable for the clinically relevant range of 1 to 10 ng/mL	Solutions and human plasma	Antibody	[70]
CEA	Paper	Ferrocyanide	Carbon ink	0.32 ng/mL	1.0–500.0 ng/mL	Solutions and human serum samples	MIP	[56]
X. fastidiosa	PDMS- glass	Ferrocyanide	Metallic microelectrodes	1×10^3 CFU/mL	1×10^3–2×10^4 CFU/mL	Leaf	Probe-free	[71]
E. coli	PDMS-glass	-	Au interdigital microelectrodes	500 CFU/mL	2×10^3–2×10^5 CFU/mL	Tap water spiked with *E. coli*	Probe-free	[72]
E. coli *P. putida* *S. epidermidis*	PDMS-glass	-	3D gold NMIs	~ 20 CFU/mL	$2 \times 10^1 - 10^5$ CFU/mL (*E. coli*) 2×10^1–10^4 CFU/mL (*P. putida*) 1×10^2–10^5 CFU/mL (*S. epidermidis*)	Synthetic urine	Probe-free	[57]
E. coli	Polyacrylate resin	Ferrocyanide	Gold	-	-	Tap water spiked with *E. coli*	Aptamer	[73]
Endotoxin	PDMS	Ferrocyanide	SPCE	500 pg/mL	500–200 ng/mL	Solutions	Aptamer	[74]
Free and total MC-LR	PDMS-glass-silicon	Ferrocyanide	Gold	5.7×10^{-10} g/L	3.3×10^{-4}–10^{-7} g/L	Drinking water and *Microcystis aeruginosa* culture	Antibody	[75]

PDMS polydimethylsiloxane, *MIPs* molecularly imprinted polymers, *NIP* nonimprinted polymer, *HAS* human serum albumin, *PMMA* poly(methyl methacrylate), *MB* methylene blue, *ssDNA* single-stranded deoxyribonucleic acid, *GST-α* glutathione-S-transferase-alpha, *FeMeOH* ferrocenemethanol, *PSA* prostate-specific antigen, *SPON2* Spondin-2, *CEA* carcinoembryonic antigen, *X. fastidiosa Xylella fastidiosa*, *E. coli Escherichia coli*, *3D gold NMIs* 3D gold nano/microislands, *SPCE* screen-printed carbon electrode, *MC-LR* microcystin-leucine arginine

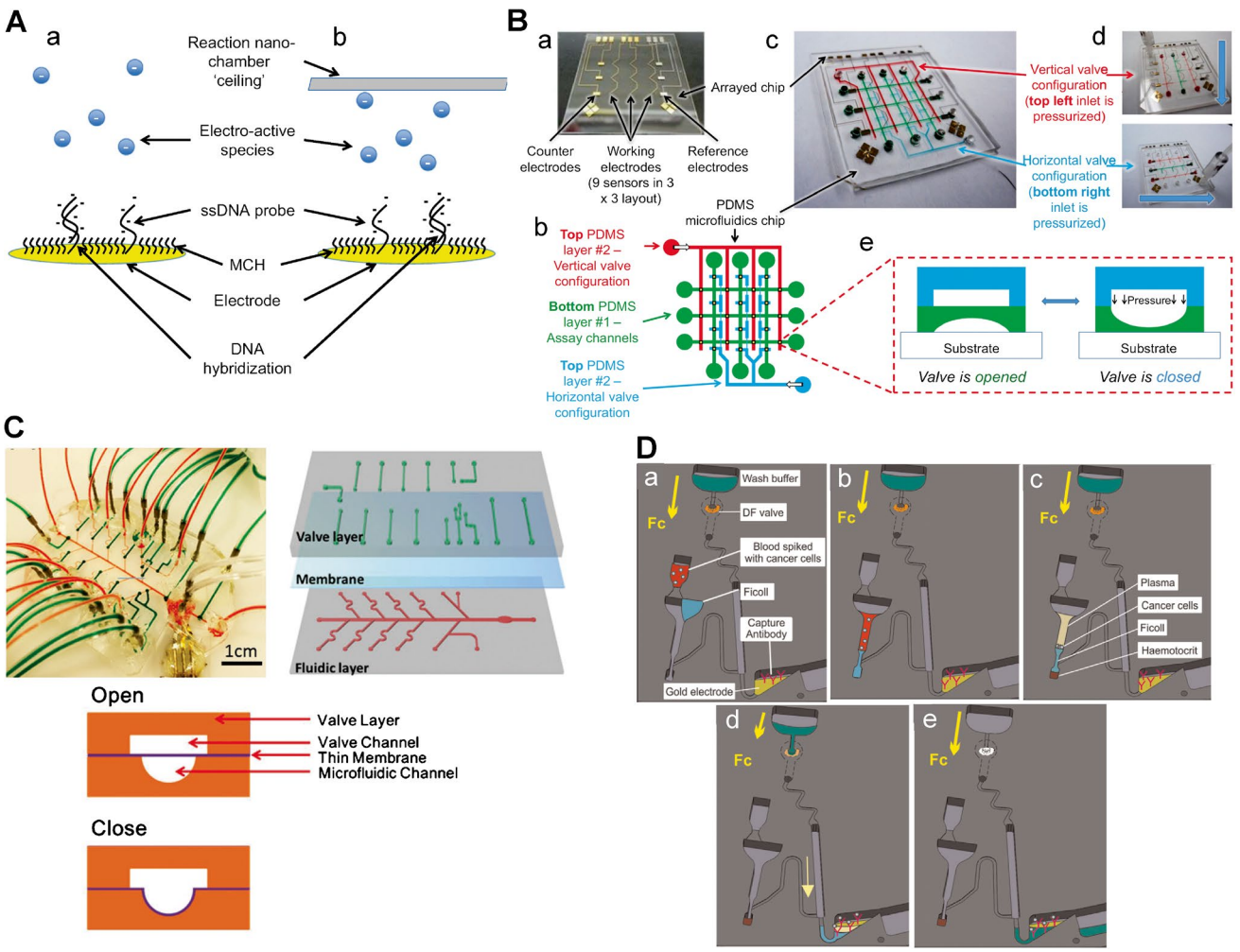

Fig. 4 Label-free impedance detection of biomarkers in a microfluidic platform. (**A**) The diffusion-based biosensing approach for (**a**) macro-scale biochips and (**b**) microfluidic-based biochips with the reflective boundary provided in the microfluidic biochips. Adapted with permission from [9]. (**B**) Microfluidic valved chip, showing (**a**) the fabricated arrayed electrochemical chip, (**b**) top valve configuration and the bottom assay channels, (**c**) entire assembled device, (**d**) vertical (top) and horizontal (bottom) valve configurations, and (**e**) valve actuation via the hydraulic channel to pinch off the microfluidic assay channel. Adapted with permission from [53]. (**C**) Three-layered microfluidic chip formed of the valve channel layer, thin membrane, and microfluidic channel, showing the push-down thin membrane for closing and opening the microfluidic channel. Adapted with permission from [12]. (**D**) Centrifugal microfluidic platform, showing (**a**) different regions on the disc, (**b**) sample layered over Ficoll at 600 rpm, (**c**) blood fractionation completed at 1500 rpm, and cancer cells layered at the interface between the Ficoll layer and the plasma, (**d**) siphon priming and extraction of the target cells, and (**e**) wash buffer released and subsequent electrochemical impedance detection. The centrifugal force direction, as indicated by the arrows. Adapted with permission from [54]

example, a silicon nanowires field-effect transistor (SiNW-FET) microfluidic device, with an active redox system consisting of 9,10-dihydroxyanthracene/9,10-anthraquinone, was developed to monitor the metabolic activity of biofilms based on glucose consumption in high-ionic-strength solutions. This nanobiosensor could monitor the production of H_2O_2 from glucose under enzymatic oxidase reactions. Thus, the nanobiosensor was proposed as an automated, label-free, real-time, and sensitive system for the detection of metabolites in very low samples in the natural environment (Fig. 3C) [47].

Electrochemical impedance spectroscopy

According to Ohm's law, the ratio of voltage to current ($Z = V/I$) is called electrical impedance (Z) [48]. In EIS, this physical variable has been applied to monitor the surface impedance alterations from the binding of a target molecule to an immobilized probe at the electrode's surfaces [49]. This approach has several advantages, including cost-efficiency, miniaturization, low power consumption, and label-free operation (Table 2). Therefore, EIS biosensors exhibit impressive potential in POC and other applications.

Table 3 Selected microfluidic label-free voltammetric biosensors

Analytes	Materials	Electroactive species	Electrode type	LOD	Linear range	Sample	Probe	Ref
Glucose	Paper	Ferrocyanide	Gold	0.11 mM	0.1–15 mM	Real food samples	GOx	[76]
Diazepam	Paper	-	Gold	1.5 nM	3.5 nM to 3.5 mM	Urine	Probe-free	[77]
WFS	PMMA	-	NPAMW	8×10^{-12} M	2×10^{-11}–4×10^{-9} M	Rabbit plasma	MIP	[78]
S. aureus and *E. coli*	Polymer films, PC, glass	Hoechst	Gold	10 CFU (*S. aureus*) 100 CFU (*E. coli*)	1.0×10^{1}–10^{6} CFU	Milk	-	[79]
E. coli	PDMS, glass	Hoechst	Carbon electrodes	24 CFU/mL	-	Urine	-	[80]
S. typhimurium	Silicon, PMMA	-	Carbon nanowires	10 CFU/mL	-	Bacterial suspensions	Aptamer	[81]
LP	-	Ferrocyanide	SPCE	10 CFU/mL	10 to 10^{8} CFU/mL	Water samples	Antibody	[82]
CEA	Paper	Thi	SPCE	10 pg/mL	50–500 pg/mL	Solutions and serum	Antibody	[83]
NSE	Paper	Thi	SPCE	10 pg/mL	1 to 500 ng/mL	Solutions and serum	Antibody	[84]
PSA	Paper	Thi	SPCE	10 pg/mL	0.05 to 200 ng/mL	Solutions and serum	Aptamer	[85]
17β-E2	Paper	NMB	SPCE	5 pg/mL	10–500 pg/mL	Solutions and serum	Aptamer	[86]
CEA CA19-9 H.P P53 PG-I PG-II	PDMS, glass	Ferrocyanide	Au microelectrodes	0.37 ng/mL (CEA) 10.75 U/mL (CA19-9) 5 U/L (HP) 35 pg/mL (P53) 37.5 ng/mL (PG I) 2.5 ng/mL (PG II)	0.37–90 ng/mL (CEA) 10.75–172 U/mL (CA19-9) 10–160 U/L (H.P.) 35–560 ng/mL (P53) 37.5–600 ng/mL (PG I) 2.5–80 ng/mL (PG II)	Solutions	Antibody	[87]
Ferritin	PMMA	Ferrocyanide	SPCE	0.413 ng/mL	7.81–500 ng/mL	Solutions and serum	Antibody	[88]
Total Hb and HbA_{1C}	Plastic	TBO	SPCE	82 nM (Hb) 3.7 nM (HbA1C)	0.1–10 µM (Hb) 0.006–0.74 µM (HbA1C)	Solution	Aptamer	[89]
Total Hb and HbA_{1C}	Glass	NB	SPCE	$8.1 \times 10^{-7} \pm 3.0 \times 10^{-8}$ (Hb) $9.2 \times 10^{-7} \pm 5 \times 10^{-8}$ (HbA1c)	1.0×10^{-6}–3.5 mM (Hb) 3.0×10^{-6}–0.6 mM (HbA1c)	Standard sample	-	[62]
OA	PDMS	Ferrocyanide	SPCE	8 pM	10–250 nM	Solutions and mussel	Aptamer	[90]
Cortisol	Glass-quartz	Triam	GCE	10 pg/mL	10 µg/mL to 30 pg/mL	Solutions and serum	Aptamer	[59]
CEA and NSE	Paper	Thi	SPCE	2 pg/mL (CEA) 10 pg/mL (NSE)	0.01–500 ng/mL (CEA) 0.05–500 ng/mL (NSE)	Solutions and serum	Aptamer	[83]
FB1 and DON	PDMS, glass	Ferrocyanide	ITO	97 pg/mL (FB1) 35 pg/mL (DON)	0.3 to 140 ppb (FB1) 0.2 to 60 ppb (DON)	Solutions and real food matrix	Antibody	[91]
cMb	PDMS, glass	Ferrocyanide	Au electrode	4 pg/mL	0.004–1000 ng/mL	Solutions and serum	Antibody	[92]

Table 3 (continued)

Analytes	Materials	Electroactive species	Electrode type	LOD	Linear range	Sample	Probe	Ref
UA and CNN	Paper	HexRu (II/III) for UA	SPCE	8.4 nM (UA) 3.7 nM (CNN)	0.01–3.0 nM (UA) 0.01–3.0 nM (CNN)	Urine	Direct UA oxidation and creatininase	[93]
MTX LDH UA Urea	Photosensitive resin	Ferrocyanide for MTX NAD for LDH MB for UA and urea	SPE	35 nM (MTX) 25 U/L (LDH) 450 nM (UA) 20 µM (Urea)	0.1–1000 µM (MTX) 60–700 U/L (LDH)	Solutions and rabbit plasma	Probe-free and urease	[94]
BPA	Paper	Ferricyanide	MWCNT printed electrode	0.35 µM	10 µM to 5 mM	Solutions	Probe-free	[61]

GOx glucose oxidase, *A* adiponectin, *L* leptin, *MIPs* molecularly imprinted polymers, *WFS* warfarin sodium, *PMMA* poly(methyl methacrylate), *NPAMW* nanoporous Au–Ag alloy microwire, *S. aureus Staphylococcus aureus*, *E. coli Escherichia coli*, *PC* polycarbonate, *CFU* colony-forming unit, *PDMS* polydimethylsiloxane, *S. typhimurium Salmonella typhimurium*, *LP Legionella pneumophila*, *SPCE* screen-printed carbon electrode, *cTnI* cardiac troponin I, *ITO* indium tin oxide, *GCE* glassy carbon electrode, *CEA* carcinoembryonic antigen, *Thi* thionine, *NSE* neuron-specific enolase, *PSA* prostate-specific antigen, *17β-E2* 17β-estradiol, *NMB* new methylene blue, *CA19-9* carbohydrate antigen 19–9, *HP Helicobacter pylori* CagA protein, *P53* P53 oncoprotein, *PG I* pepsinogen I, *PG-II* pepsinogen II, *Hb* hemoglobin, HbA_{1C} glycated hemoglobin, *NB* Nile blue, *TBO* toluidine blue O, *OA* Okadaic acid, *Triam* triamcinolone, *FB1* fumonisin B1, *DON* deoxynivalenol, *cMb* cardiac myoglobin, *UA* uric acid, *CNN* creatinine, *HexRu(II/III)* hexaammineruthenium (II/III), *MTX* methotrexate, *LDH* lactate dehydrogenase, *NAD* nicotinamide adenine dinucleotide, *MB* methylene blue, *SPE* screen-printed electrodes, *BPA* bisphenol A, *MWCNT* multiwall carbon nanotube-printed electrode

Quantification and detection of molecules with EIS experience a growing demand in clinical diagnostics [50, 51] including molecular screening [52]. EIS is one of the commonly used powerful methods to characterize the hybridization of DNA, whose interaction with its immobilized probe on the electrode surface repels negative electroactive species and affects its diffusion features. The miniaturization of the reaction chamber volume to a nanoscale can enhance the effect of diffusion on the sensing mechanism. It amplifies the biosensing signal that in turn improves the LOD (Fig. 4A) [9]. A lab-on-a-chip (LOC) device with an array of separately addressable reaction chambers for the label-free diffusion-restricted electrochemical analysis of DNA hybridization events has been developed. This microfluidic LOC consists of two microchannel layers made of PDMS, in which the top and bottom layers include valves and assay channels, respectively. This valve-based manipulation microsystem was found to improve the repeatability and experimental control. Further, a conventional redox couple ($[Fe(CN)_6]^{4-/3-}$) was used to characterize the electrochemical performance of the device (Fig. 4B) [53].

It should be noted that the establishment of competent biosensing platforms capable of accurate, long-term, and continual monitoring of biomarkers and cell population dynamics is required to evaluate the tissue or cell biological response. Shin and coworkers have developed the label-free microfluidic electrochemical biosensor integrated with a human organoid system for the continual and automated analysis of cell-secreted soluble biomarkers [12]. The GST-α and albumin were label-free detected using EIS technique with the LOD of 0.01 and 0.023 ng/mL, respectively. Microfluidic valves' utilization on this chip allows automated detection and regeneration processes without compromising the sensor sensitivity for up to 1 week, where a systemically applied drug changes the organoids' metabolic activity (Fig. 4C).

To combine the advantages of lab-on-a-disc (LoaD) platforms and EIS, a highly sensitive label-free electrochemical system was designed to detect ovarian cancer cells from the whole blood in a fully integrated, automated, multiplexed fashion [54]. The combination of capillary-based siphon valving strategy with the centrifuge-pneumatic dissolvable-film valves was used for the automated sample preparation. The assay was conducted in the absence of an external pumping device. The anti-EpCAM was immobilized on the self-assembled L-cysteine on the gold electrode as a bioreceptor. The LOD for detecting ovarian cancer cells was about 214 captured cells/mm^2, and the capture efficiency was about 87%. The buffer electrolyte concentration was adjusted to extend the thickness of the electrical double layer; hence, the bound cells could interact with the interfacial electric field. This electrochemical LoaD platform was shown to parallelly conduct five different analyses with a linear dynamic range

between 16,400 and $(2.6 \pm 0.0003) \times 10^6$ cancer cells/mL of blood. It was proposed as the prognostic tool in clinical settings, in which the minimum preparation of the sample and easy handling are the keys (Fig. 4D).

A POC label-free approach has been described based on the EIS microfluidic paper-based analytical device (μPAD) for the detection of intact virus particles at clinically relevant concentrations in a short few minutes. The electrode surface's impedance was significantly changed by the interaction of the virus with the Ab molecules' functionalized Au microwires. Additionally, the use of a microfluidic platform instead of a classical paper-based structure was shown to significantly improve the LOD because of the improved mass transport and particles capturing on the modified electrodes [55]. Besides, multiplex POC devices have been developed for the simultaneous detection of cancer-specific biomarkers [33]. A paper-based microfluidic device with in situ synthesized MIPs and a movable valve was developed for the electrochemical detection of carcinoembryonic antigen (CEA) using a convenient and continuous flow of fluid through the movable valves, which significantly enhanced the performance during the synthesis of dopamine MIP layer and biomarker detection [56]. Microfluidic devices have been used for the label-free detection of bacteria with EIS techniques in agricultural settings and clinical practice. Several types of bacteria with different morphology (*Pseudomonas putida*, *Escherichia coli* K12, and *Staphylococcus epidermidis*) were successfully distinguished based on their different electron charge transfer. The label-free impedimetric detection was performed in the absence of biological receptors such as antibodies or DNA in a portable fashion and a short time of 10 min. The proposed platform detected dilutions as low as ~ 20 CFU/mL in a wide linear range of detection of 2.0×10^1–10^4, 2.0×10^1–10^5, and 1.0×10^2–10^5 CFU/mL for *P. putida*, *E. coli*, and *S. epidermidis*, respectively [57]. A nanobridge-based interdigitated electrode (IDE) sensor was developed for ultrasensitive detection of multiple forms of free radicals from various sources, including UV radiation, Fenton reaction, and cigarette smoke. The nanobridges were placed among the IDEs, which comprised the long single-strand DNA and wrapped around multiwalled carbon nanotubes (MWCNTs). The proposed IDE sensor was successfully used to detect the mechanism of DNA damage and/or cleave due to the free radicals' attack [58].

Electrochemical voltammetry

The principle of label-free voltammetric biosensing is based on the measurement of generated current from the redox reaction of electroactive species at a variable potential [14]. The voltage is applied between the working and reference electrodes, while the current is measured between the working and counter electrodes. The data are plotted as current intensity versus voltage (the so-called voltamperogram). Several forms of voltammetry based on potential alteration manner have been introduced and applied in electrochemical sensing. These include linear sweep voltammetry, cyclic voltammetry (CV), differential pulse voltammetry (DPV), and square wave voltammetry (SWV) (Table 3).

An electrochemical microfluidic device was developed for the detection of cortisol in serum and saliva samples without washing steps and labeling the target [59]. Gold nanoparticle (AuNP)/graphene-modified glassy carbon electrodes were used as a platform. Ap-functionalized AuNPs with high surface areas were employed to enhance the analyte's capture under a 3D diffusion profile. Triamcinolone (TA), as the electro-active cortisol mimicking molecule, was pre-bound to the Ap in the presence of cortisol. Upon the analysis, the TA displacement from the Ap by cortisol and the SWV current was enhanced. Altogether, the cortisol concentration acquired from this device was found to be comparable with those achieved from other available conventional methods such as ELISA. However, the proposed method was operational with significantly smaller sample volumes (< 1 μL) and a much shorter assay time of 2.5 min in comparison to the few hours required for ELISA (Fig. 5A).

A highly sensitive label-free electrochemical μPAD was developed to detect CEA in standard and clinical serum samples [60]. The wax- and screen-printing methods were used to fabricate the microfluidic channels and electrodes, respectively. The screen-printed carbon working electrode was modified using amino-functional graphene (NG)/thionine (Thi)/AuNP nanocomposites to increase the sensitivity of the immunosensor. Thionine can generate a current at certain potentials. By forming antibody-antigen immunocomplex, the response currents were decreased with the CEA concentrations. The linear ranges of 50 pg/mL to 500 ng/mL and the LOD of 10 pg/mL (S/N = 3) were obtained under optimum conditions. Hence, this μPAD would provide a platform with high efficiency, low cost, and reagent volume for specific, sensitive, and POC detection of cancer biomarkers (Fig. 5B).

Dual detection of bisphenol A on μPAD was recently proposed based on the laser desorption ionization mass spectrometric (LDI-MS) and electrochemical detection [61]. The fabricated device could readily deliver the fluid samples to both detection zones without using an external pump. Two ballpoint pens filled with MWCNTs and silver nanoparticles (AgNPs) ink and plotters were used to print the electrochemical sensor. To further improve the sensitivity, zinc oxide (ZnO) was used to modify the LDI-MS and electrochemical detection zones. Compared to the conventional organic matrix, ZnO can change the interferences and enhance the electron transfer in LDI-MS and electrochemical sensing improving the ionization efficiency. This platform provided a dual detection possibility with a LOD of about 0.01 pM for LDI-MS and 0.35 μM for electrochemical detection under optimal conditions. The detection methods can parallelly be applied to improve precision and confidence by utilizing a single portable device.

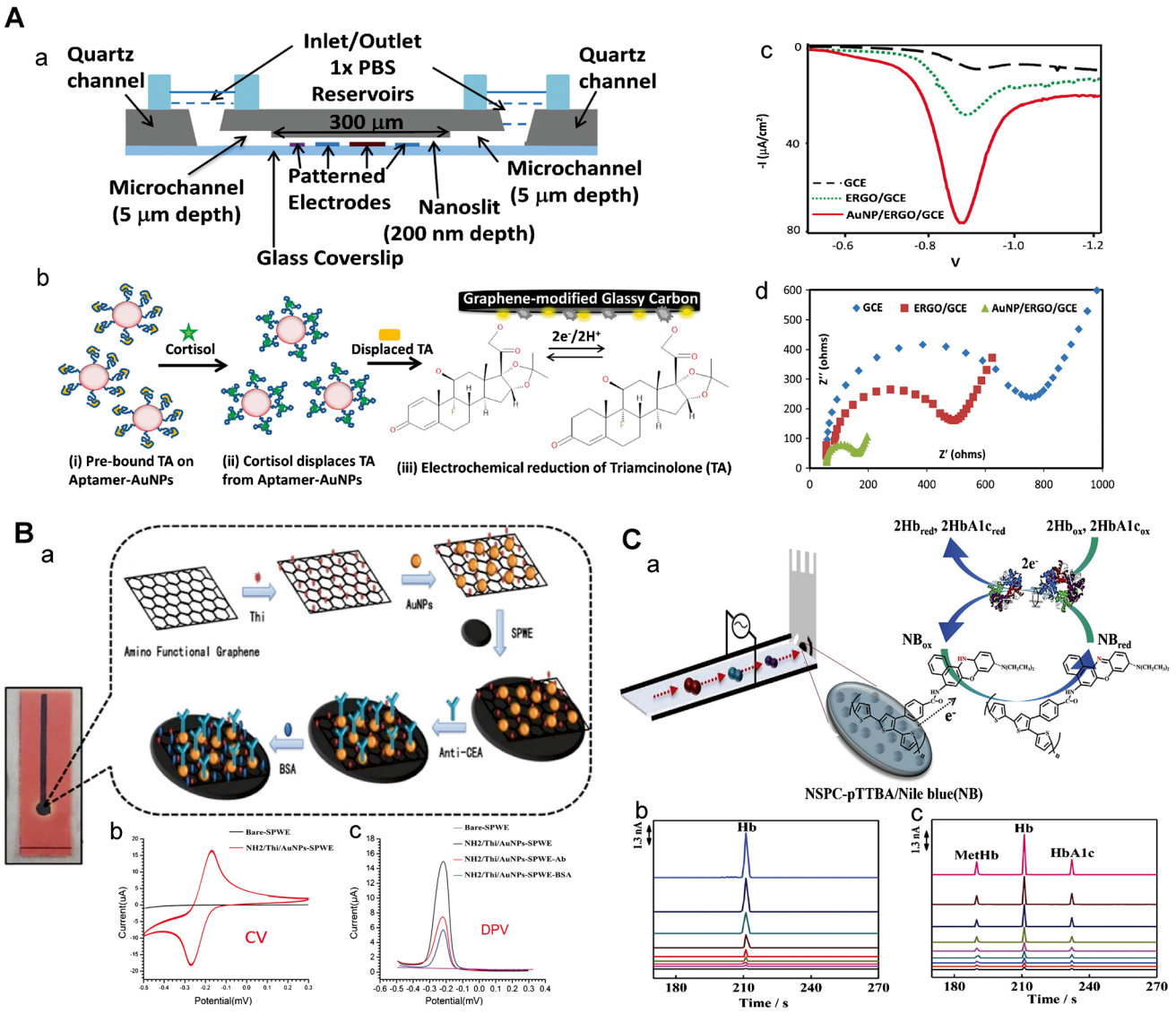

Fig. 5 (**A**) The schematic presentation of patterned electrodes on a glass coverslip within a SU8 layer, showing (**a**) a cross-sectional view of the nanoslit geometry, (**b**) the signal from electrochemical reduction of triamcinolone used for aptamer-based cortisol detection, (**c**) enhanced square wave voltammetric signal at glassy carbon electrode versus nanomaterial modified electrodes composed of ERGO with AuNPs, and (**d**) RCT resistance at graphene-modified (AuNP/ERGO) electrodes versus GCE. Adapted with permission from [59]. (**B**) The preparation procedure of (**a**) N-G/Thi/AuNPs nanocomposites on the screen-printed working electrode using paper and its modification procedure, which was assessed through (**b**) CV, and (**c**) DPV. Adapted with permission from [60]. (**C**) Hb and HbA1c sensor fabrication and the detection method, showing (**a**) schematic illustration of the device, (**b** and **c**) electropherograms obtained for varying concentrations of (**a**) Hb, and (**c**) HbA1c. Adapted with permission from [62]. NG/Thi/AuNPs: amino-functional graphene/thionine/gold nanoparticles, ERGO: electrochemically reduced graphene oxide, AuNPs: gold nanoparticles, RCT: reduction in charge transfer, CV: cyclic voltammetry, DPV: differential pulse voltammetry, LDI-MS: laser desorption ionization mass spectrometric, Hb: hemoglobin

The combination of electrochemical detection with separation channels is a promising approach for POC analysis. An amperometric sensor coupled with an electrochemical AC field applied-microfluidic device was fabricated for simultaneous detection of hemoglobin (Hb) and glycated hemoglobin (HbA1c) in human blood samples (Fig. 5C). The device was developed based on the immobilization of Nile blue (NB) as a catalytic redox mediator on the conductive polymer chain of poly(2,2′:5′,2″-terthiophene-3′-p-benzoic acid) (pTTBA) interspersed with N, S-doped porous carbon (NSPC) nanocomposite layer. The developed microfluidic sensor provided fast and sensitive measurement in the absence of biological receptors (enzyme, Ab, Ap, etc.) with linear dynamic ranges of 1.0×10^{-6} to 3.5 mM and 3.0×10^{-6} to 0.6 mM, together with the LOD of

Table 4 Selected microfluidic label-free chronoamperometric biosensors

Analytes	Materials	Electroactive species	Electrode type	LOD	Linear range	Sample	Probe	Ref
Glucose	PDMS, glass, silicone	H_2O_2	DLC thin film electrodes	0.5 mM	Up to 12 mM	Standard sample	GOx	[95]
Glucose	Paper	FCA	SPCE	0.03 mM	0.1 to 40 mM	Urine	GOx	[96]
H_2O_2	Glass	-	Gold micro-electrode	20 nM	100 nM–20 mM	Standard sample	CONSs	[97]
Alcohol, vitamins, glucose	Polycarbonate, paper	PB	SPE/carbon-PB ink (alcohol) SPE/GOx-PB ink (glucose) Bare SPE (vitamins)	-	-	Tear	AOx and GOx	[63]
Lactate glucose	Silicone, PMMA, PDMS	PB	LOx and GOx modified PB electrodes	50 µM for Glc	-	Sweat	LOx and GOx	[98]
Melatonin	PDMS	Ferricyanide	SPE	20 pg/mL	-	Urine	MIP	[99]
Alcohol	PMMA, PDMS, silicon	TMB	Pt electrodes	4.5 nA	0–1.25 g/L	Whole blood	AOx and HPR	[100]
Creatinine	Paper	-	SPCE	0.22 mM	0.01–2.0 mM	Serum	Probe-free	[64]
Glucose	Paper	Ferricyanide	SPCE	0.33 mM	0.5–50 mM	Standard sample	FAD-dependent GDH	[101]
Glucose	PDMS	H_2O_2	Pt-black micro-electrode	0.05 mM	0.2–43.5 mM	Serum	GOx	[102]
Glucose	PDMS	Ferricyanide	NPG electrode	-	0.01–1 mM	Sweat	Probe-free	[65]
H1N1 virus	PDMS, glass	Ferricyanide	Gold	0.5 PFU/mL	$1–10^4$ PFU/mL	Standard sample	Antibody	[66]

PDMS polydimethylsiloxane, *GOx* glucose oxidase, *DLC* diamond-like carbon, *SPCE* screen-printed carbon electrode, *FCA* ferrocenecarboxylic acid, *CONS* cerium oxide nanosheets (exhibit triple-enzyme mimetic activity), *PMMA* poly(methyl methacrylate), *PB* Prussian blue, *AOx* alcohol oxidase, *Lox* lactate oxidase, *SPE* screen-printed electrode, *MIP* molecularly imprinted polymer, *TMB* tetramethylbenzidine, *HPR* horseradish peroxidase, *BChE* butyrylcholinesterase enzyme, *FAD* flavin adenine dinucleotide, *GDH* glucose dehydrogenase, *ITO* indium tin oxide, *NPG* nanoporous gold

$8.1 \times 10^{-7} \pm 3.0 \times 10^{-8}$ and $9.2 \times 10^{-7} \pm 5 \times 10^{-8}$ mM for Hb and HbA1c, respectively [62].

Chronoamperometry technique

Chronoamperometry (CHA) is a time-dependent voltammetric technique, which has been used as a sensing technique in label-free detection solely or together with other electrochemical techniques such as CV. CHA is one of the simplest electrochemical methods, which is an ideal approach for POC application and as a model detection method (Table 4). An eyeglass-based microfluidic electrochemical device was designed for noninvasive label-free monitoring of different targets such as glucose, alcohol, and vitamins in tears [63]. This wearable microfluidic system can be placed outside the eye region. It can be used for real-time tear collection and monitoring of biomarkers, which can eliminate the drawbacks of direct contact of the sensor systems with the eye (Fig. 6A). The rapid digital dispensing approach was applied to dispense copper oxide-ionic liquid composite (CuO-IL) onto an electrochemically reduced graphene-modified screen-printed carbon electrode (ERGO/SPCE). As shown in Fig. 6B, the paper-based sensor demonstrated a linear range of 0.01–2.0 mM and the LOD of 0.22 µM for creatinine [64]. A variety of label-free CHA microfluidic sensors has been developed to determine glucose in the healthcare fields, foods, and beverage industries. For instance, a wearable microfluidic electrochemical glucose sensor was reported for monitoring daily sweat glucose using nanoporous gold (NPG) electrochemical biosensor [65]. The NPG electrodes possessed a high surface area, high electrochemical catalytic effect, and outstanding chemical stability. As a result, an NPG working electrode, an Au counter, and Ag/AgCl reference electrode were patterned on the 3D micropatterned PDMS substrate to provide the sensitivity and mechanical stretchability in the nonenzymatic detection of glucose. The 3D micropatterned PDMS substrate was used as a stress-absorbing layer during stretching. The microfluidic NPG sensor exhibited accurate and continuous monitoring of the sweat glucose level with high selectivity and sensitivity (i.e., 253.4 µA/cm^2/mM), mechanical

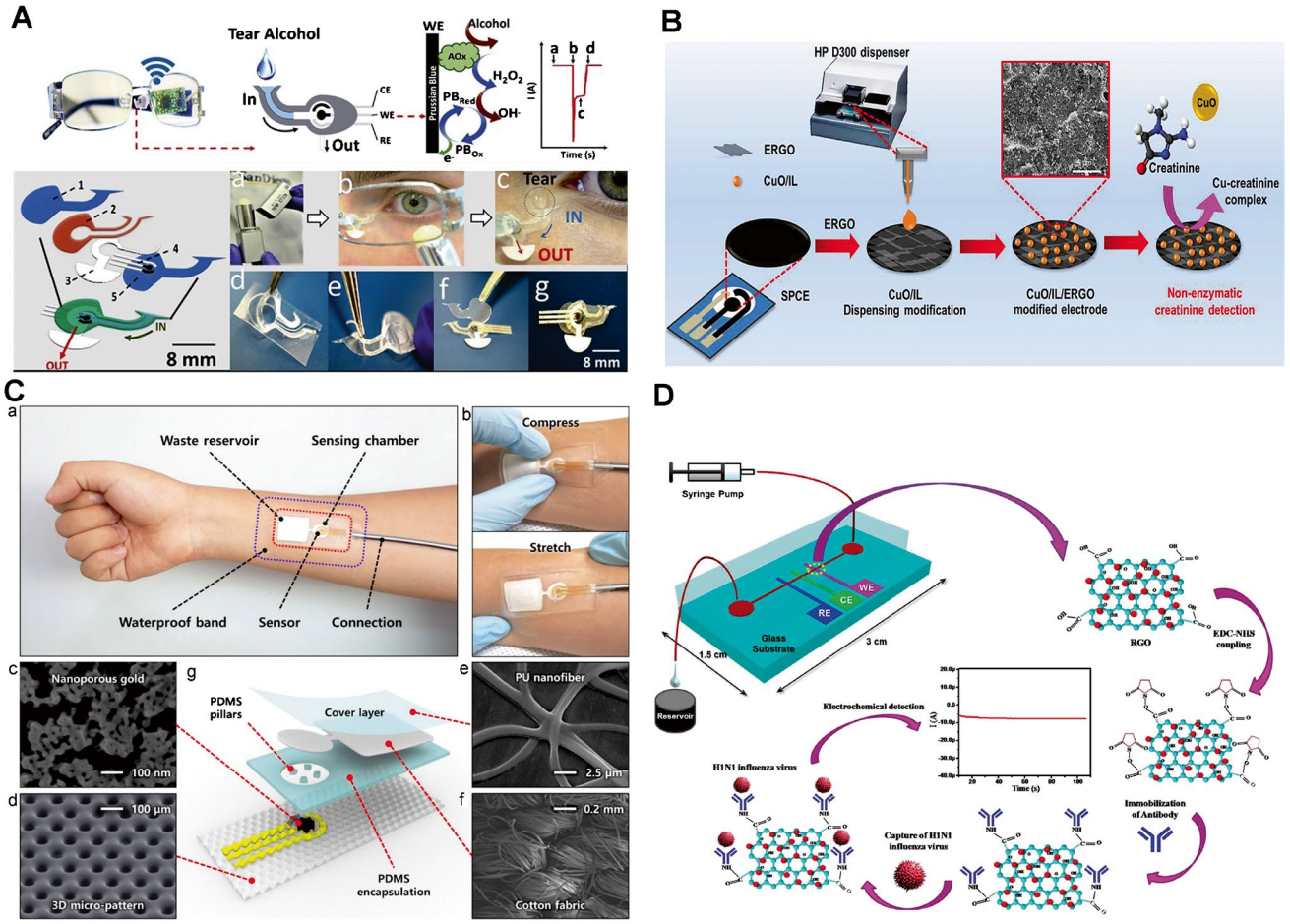

Fig. 6 (**A**) Eyeglass-based microfluidic system, integration of fluidic device, and wireless electronics as the eyeglasses with enzymatic alcohol detection and signal transduction, in which (**a**) corresponds to the baseline, (**b**) current change as a result of the captured tear, (**c**) the measured alcohol signal, and (**d**) drying of the device. (**B**) A structured view of the microfluidic system showing (1) top polycarbonate membrane, (2) double-adhesive spacer, (3) paper outlet, (4) electrochemical sensing system, and (5) bottom polycarbonate membrane. The photos of (**a**) the tear stimulation menthol tear stick, (**b**) the volunteer applying the tear stick under the left eye, and (**c**) the entrance of the tear into the inlet. The fabrication of the fluidic device through (**d**) adhesive spacer removal from the PET substrate, (**e**) spacer placement on the bottom membrane, (**f**) placement of electrode and outlet on top of the spacer followed by the top membrane, and (**g**) mounted device on eyeglasses nose-bridge pad. Adapted with permission from [63]. (**B**) Digital dispensing in the fabrication of CuO-IL/rGO composite for nonenzymatic creatinine determination on the paper-based microfluidic sensor in human blood serum. Adapted with permission from [64]. (**C**) The structural representation of the fully stretchable microfluidic-integrated biosensor patch on the skin, showing (**a**) the fabricated patch mounted on the human skin, (**b**) conformality of the patch, (**c**) FE-SEM micrograph of NPG electrochemical electrode (top view), (**d**) 3D micropatterned PDMS substrate, (**e**) PU nanofiber, (**f**) stretchable cotton fabric, and (**g**) the layered structure of the microfluidic-integrated biosensor patch. Adapted with permission from [65]. (**D**) Integration of electrochemical immunosensor with a microfluidic chip for the influenza virus H1N1 detection. Adapted with permission from [66]

durability, precise sample handling, and no degradation after 1000 cycles of stretching to 30% strain (Fig. 6C) [65]. Singh and colleagues reported a reduced graphene oxide (rGO)-based electrochemical microfluidic device for the label-free detection of an influenza virus, H1N1 strain. The rGO sheets were used to increase the loading capacity of Abs onto the electrode surface through covalent bonding between the carboxyl end of the rGO and the Ab. Ab molecules were immobilized via EDC/NHS conjugation chemistry. Three microelectrodes were built on a glass material and encapsulated with a PDMS microchannel. This device displayed good selectivity and sensitivity towards the H1N1 strain. The CHA current was raised by increasing the concentration of the virus within the linear range of 1 to 104 PFU/mL and the LOD of 0.5 PFU/mL (Fig. 6D) [66].

Scientific and technical challenges

Before their translation into clinical applications, some imperative scientific and technical challenges of microfluidic-based systems should be fully addressed. These may include (i) material limitations (e.g., sensitivity/

quantitation issues in paper-based diagnostics), (ii) issues related to the continuous flow microfluidic-based sensing systems, (iii) variation in the functions/behavior of fluids containing reagents, (iv) inconsistency in terms of interchangeable parts, (v) custom calculations necessary for the modular systems, and (vi) issues related to the integration and function of electrodes [67]. Further, the scale-dependent effect concerning the Reynolds number operation might compromise the applicability of the device. Altogether, microfluidic sensing devices are delicate systems that need several optimization processes to assure the accuracy and reproducibility of the whole system.

Conclusions and future perspectives

Microfluidic-based research has dramatically advanced since its introduction and integration with electrochemical detection methods. The label-free methods, in particular, offer robust tools combining different components into a single platform to replace the bulky traditional instruments. The recent advancements in microfluidic fabrication materials and developments in label-free electrochemical microfluidic devices have highlighted their potential as POC systems. Silicon and glass have notable applications in the early developments of microfluidic systems; however, they can hardly be used in the construction of active fluidic units such as pumps and valves. Polymeric materials, PDMS in particular, have gradually become much more popular, especially in developing disposable and low-cost microfluidic devices. While glass/silicon and PDMS materials are commonly utilized for research purposes, paper is used as a well-suited material for the fabrication of microdevices in resource-limited settings and commercial fluidic devices. Moreover, paper-based microdevices, which are simple, cost-efficient, and disposable, do not require an external pump. Label-free electrochemical microfluidic devices provide substantial analytical properties and are promising candidates for clinical diagnostics. They offer valuable advantages in efficiency and cost by simplifying the procedure, reagent consumption, convenience, and analysis time. Many of the devices mentioned in this review enable sensitive, specific, and low-cost detection of clinically relevant and valid markers. However, several challenges (e.g., the selectivity of the test in complex matrix samples) must be overcome before the POC diagnostics can be implemented. MESDs can be applied in various crucial fields such as biomedical studies, environmental monitoring, and POC diagnostics. Nonetheless, some issues (e.g., precision, sensitivity, range, manufacturing cost, and user-friendly applications) might potentially limit the development and translation of the POC systems into real-world applications. So far, some progress has been made in multiplex analyses through microfluidic technology because of the multimarker basis of most diseases, while many advancements need to take place to assure the applicability and precision of the analytical devices. Moreover, it should be noted that the selection of the right methodologies might improve the sensitivity, portability, and rapid detection of the MESDs. Collectively, we envision that the simplified multiplex detection of analytes in complex settings will be the center of mainstream analytical sensing and monitoring with possible emerging applications in processing living cells, tissues, and organs.

Funding The authors like to acknowledge the Research Center for Pharmaceutical Nanotechnology at Tabriz University of Medical Sciences for supporting this PhD thesis (# 63766).

Declarations

Conflict of interest The authors declare no competing interests.

References

1. Whitesides GM (2006) The origins and the future of microfluidics. Nature 442:368–373. https://doi.org/10.1038/nature05058
2. Mou L, Jiang X (2017) Materials for microfluidic immunoassays: a review. Adv Healthc Mater 6:1601403. https://doi.org/10.1002/adhm.201601403
3. Miao Q, Qi J, Li Y, Fan X, Deng D, Yan X et al (2021) Anchoring zinc-doped carbon dots on a paper-based chip for highly sensitive fluorescence detection of copper ions. Analyst 146:6297–6305. https://doi.org/10.1039/d1an01268a
4. Amirifar L, Besanjideh M, Nasiri R, Shamloo A, Nasrollahi F, de Barros NR et al (2022) Droplet-based microfluidics in biomedical applications. Biofabrication 14:022001. https://doi.org/10.1088/1758-5090/ac39a9
5. Rettke D, Danneberg C, Neuendorf TA, Kuhn S, Friedrichs J, Hauck N et al (2022) Microfluidics-assisted synthesis and functionalization of monodisperse colloidal hydrogel particles for optomechanical biosensors. J Mater Chem B. https://doi.org/10.1039/d1tb02798k
6. Zhu C, Maldonado J, Sengupta K (2021) CMOS-based electrokinetic microfluidics with multi-modal cellular and biomolecular sensing for end-to-end point-of-care system. IEEE Trans Biomed Circuits Syst 15:1250–1267. https://doi.org/10.1109/TBCAS.2021.3136165
7. Zhang S, Zahed MA, Sharifuzzaman M, Yoon S, Hui X, Chandra Barman S et al (2021) A wearable battery-free wireless and skin-interfaced microfluidics integrated electrochemical sensing patch for on-site biomarkers monitoring in human perspiration. Biosens Bioelectron 175:112844. https://doi.org/10.1016/j.bios.2020.112844
8. Vasudev A, Kaushik A, Tomizawa Y, Norena N, Bhansali S (2013) An LTCC-based microfluidic system for label-free, electrochemical detection of cortisol. Sens Actuators B Chem 182:139–146. https://doi.org/10.1016/j.snb.2013.02.096
9. Ben-Yoav H, Dykstra PH, Bentley WE, Ghodssi R (2012) A microfluidic-based electrochemical biochip for label-free

diffusion-restricted DNA hybridization analysis. Biosens Bioelectron 38:114–120. https://doi.org/10.1016/j.bios.2012.05.009
10. Labib M, Sargent EH, Kelley SO (2016) Electrochemical methods for the analysis of clinically relevant biomolecules. Chem Rev 116:9001–9090. https://doi.org/10.1021/acs.chemrev.6b00220
11. Felix FS, Angnes L (2018) Electrochemical immunosensors–a powerful tool for analytical applications. Biosens Bioelectron 102:470–478. https://doi.org/10.1016/j.bios.2017.11.029
12. Shin SR, Kilic T, Zhang YS, Avci H, Hu N, Kim D et al (2017) Label-free and regenerative electrochemical microfluidic biosensors for continual monitoring of cell Secretomes. Adv Sci 4:1600522. https://doi.org/10.1002/advs.201600522
13. Yu X, Xu D, Cheng Q (2006) Label-free detection methods for protein microarrays. Proteomics 6:5493–5503. https://doi.org/10.1002/pmic.200600216
14. Rhouati A, Catanante G, Nunes G, Hayat A, Marty J-L (2016) Label-free aptasensors for the detection of mycotoxins. Sensors 16:2178. https://doi.org/10.3390/s16122178
15. Nge PN, Rogers CI, Woolley AT (2013) Advances in microfluidic materials, functions, integration, and applications. Chem Rev 113:2550–2583. https://doi.org/10.1021/cr300337x
16. Lin C-H, Lee G-B, Lin Y-H, Chang G-L (2001) A fast prototyping process for fabrication of microfluidic systems on soda-lime glass. J Micromech Microeng 11:726. https://doi.org/10.1088/0960-1317/11/6/316
17. Washburn AL, Gunn LC, Bailey RC (2009) Label-free quantitation of a cancer biomarker in complex media using silicon photonic microring resonators. Anal Chem 81:9499–9506. https://doi.org/10.1021/ac902006p
18. Ren K, Zhou J, Wu H (2013) Materials for microfluidic chip fabrication. Acc Chem Res 46:2396–2406. https://doi.org/10.1021/ar300314s
19. Quinn DJ, Spearing SM, Ashby MF, Fleck NA (2006) A systematic approach to process selection in MEMS. J Microelectromech Syst 15:1039–1050. https://doi.org/10.1109/JMEMS.2006.880292
20. Iliescu C, Taylor H, Avram M, Miao J, Franssila S (2012) A practical guide for the fabrication of microfluidic devices using glass and silicon. Biomicrofluidics 6:016505. https://doi.org/10.1063/1.3689939
21. Nawrot W, Malecha K (2020) Biomaterial embedding process for ceramic–polymer microfluidic sensors. Sensors 20:1745. https://doi.org/10.3390/s20061745
22. Pandey CM, Augustine S, Kumar S, Kumar S, Nara S, Srivastava S et al (2018) Microfluidics based point-of-care diagnostics. Biotechnol J 13:1700047. https://doi.org/10.1002/biot.201700047
23. Herzberger J, Sirrine JM, Williams CB, Long TE (2019) Polymer design for 3D printing elastomers: recent advances in structure, properties, and printing. Prog Polym Sci 97:101144. https://doi.org/10.1016/j.progpolymsci.2019.101144
24. Becker H, Gärtner C (2008) Polymer microfabrication technologies for microfluidic systems. Anal Bioanal Chem 390:89–111. https://doi.org/10.1007/s00216-007-1692-2
25. Martinez AW, Phillips ST, Butte MJ, Whitesides GM (2007) Patterned paper as a platform for inexpensive, low-volume, portable bioassays. Angew Chem Int Ed Engl 46:1318–1320. https://doi.org/10.1002/anie.200603817
26. Jiang X, Fan ZH (2016) Fabrication and operation of paper-based analytical devices. Annu Rev Anal Chem 9:203–222. https://doi.org/10.1146/annurev-anchem-071015-041714
27. Ebrahimi M, Johari-Ahar M, Hamzeiy H, Barar J, Mashinchian O, Omidi Y (2012) Electrochemical impedance spectroscopic sensing of methamphetamine by a specific aptamer. Bioimpacts 2:91–95. https://doi.org/10.5681/bi.2012.013
28. Saberian-Borujeni M, Johari-Ahar M, Hamzeiy H, Barar J, Omidi Y (2014) Nanoscaled aptasensors for multi-analyte sensing. Bioimpacts 4:205–215. https://doi.org/10.15171/bi.2014.015
29. Johari-Ahar M, Rashidi MR, Barar J, Aghaie M, Mohammadnejad D, Ramazani A et al (2015) An ultra-sensitive impedimetric immunosensor for detection of the serum oncomarker CA-125 in ovarian cancer patients. Nanoscale 7:3768–3779. https://doi.org/10.1039/c4nr06687a
30. Fathi F, Ezzati Nazhad Dolatanbadi J, Rashidi MR, Omidi Y (2016) Kinetic studies of bovine serum albumin interaction with PG and TBHQ using surface plasmon resonance. Int J Biol Macromol 91:1045–1050. https://doi.org/10.1016/j.ijbiomac.2016.06.054
31. Majidi MR, Omidi Y, Karami P, Johari-Ahar M (2016) Reusable potentiometric screen-printed sensor and label-free aptasensor with pseudo-reference electrode for determination of tryptophan in the presence of tyrosine. Talanta 150:425–433. https://doi.org/10.1016/j.talanta.2015.12.064
32. Karami P, Majidi MR, Johari-Ahar M, Barar J, Omidi Y (2017) Development of screen-printed tryptophan-kynurenine immunosensor for in vitro assay of kynurenine-mediated immunosuppression effect of cancer cells on activated T-cells. Biosens Bioelectron 92:287–293. https://doi.org/10.1016/j.bios.2016.11.010
33. Pakchin PS, Nakhjavani SA, Saber R, Ghanbari H, Omidi Y (2017) Recent advances in simultaneous electrochemical multianalyte sensing platforms. Trends Anal Chem 92:32–41. https://doi.org/10.1016/j.trac.2017.04.010
34. Akbari Nakhjavani S, Khalilzadeh B, Samadi Pakchin P, Saber R, Ghahremani MH, Omidi Y (2018) A highly sensitive and reliable detection of CA15-3 in patient plasma with electrochemical biosensor labeled with magnetic beads. Biosens Bioelectron 122:8–15. https://doi.org/10.1016/j.bios.2018.08.047
35. Samadi Pakchin P, Ghanbari H, Saber R, Omidi Y (2018) Electrochemical immunosensor based on chitosan-gold nanoparticle/carbon nanotube as a platform and lactate oxidase as a label for detection of CA125 oncomarker. Biosens Bioelectron 122:68–74. https://doi.org/10.1016/j.bios.2018.09.016
36. Akbari Nakhjavani S, Afsharan H, Khalilzadeh B, Ghahremani MH, Carrara S, Omidi Y (2019) Gold and silver bio/nanohybrids-based electrochemical immunosensor for ultrasensitive detection of carcinoembryonic antigen. Biosens Bioelectron 141:111439. https://doi.org/10.1016/j.bios.2019.111439
37. Fathi F, Rashidi MR, Omidi Y (2019) Ultra-sensitive detection by metal nanoparticles-mediated enhanced SPR biosensors. Talanta 192:118–127. https://doi.org/10.1016/j.talanta.2018.09.023
38. Hashemzadeh S, Omidi Y, Rafii-Tabar H (2019) Amperometric lactate nanobiosensor based on reduced graphene oxide, carbon nanotube and gold nanoparticle nanocomposite. Mikrochim Acta 186:680. https://doi.org/10.1007/s00604-019-3791-0
39. Jalilzadeh-Razin S, Mantegi M, Tohidkia MR, Pazhang Y, Pourseif MM, Barar J et al (2019) Phage antibody library screening for the selection of novel high-affinity human single-chain variable fragment against gastrin receptor: an in silico and in vitro study. Daru 27:21–34. https://doi.org/10.1007/s40199-018-0233-1
40. Samadi Pakchin P, Fathi M, Ghanbari H, Saber R, Omidi Y (2020) A novel electrochemical immunosensor for ultrasensitive detection of CA125 in ovarian cancer. Biosens Bioelectron 153:112029. https://doi.org/10.1016/j.bios.2020.112029
41. Rivas L, Mayorga-Martinez CC, Quesada-González D, Zamora-Gálvez A, de la Escosura-Muñiz A, Merkoçi A (2015) Label-free impedimetric aptasensor for ochratoxin–a detection using iridium oxide nanoparticles. Anal Chem 87:5167–5172. https://doi.org/10.1021/acs.analchem.5b00890

42. Hua X, Xia H-L, Long Y-T (2019) Revisiting a classical redox process on a gold electrode by operando ToF-SIMS: where does the gold go? Chem Sci 10:6215–6219. https://doi.org/10.1039/C9SC00956F
43. Ji X, Chan PK (2017) Highly sensitive glucose sensor based on organic electrochemical transistor with modified gate electrode. Springer, Biosensors and Biodetection, pp 205–216
44. Pappa AM, Curto VF, Braendlein M, Strakosas X, Donahue MJ, Fiocchi M et al (2016) Organic transistor arrays integrated with finger-powered microfluidics for multianalyte saliva testing. Adv Healthc Mater 5:2295–2302. https://doi.org/10.1002/adhm.201600494
45. Lin P, Luo X, Hsing IM, Yan F (2011) Organic electrochemical transistors integrated in flexible microfluidic systems and used for label-free DNA sensing. Adv Mater 23:4035–4040. https://doi.org/10.1002/adma.201102017
46. Zhang G-J, Chua JH, Chee R-E, Agarwal A, Wong SM (2009) Label-free direct detection of MiRNAs with silicon nanowire biosensors. Biosens Bioelectron 24:2504–2508. https://doi.org/10.1016/j.bios.2008.12.035
47. Yeor-Davidi E, Zverzhinetsky M, Krivitsky V, Patolsky F (2020) Real-time monitoring of bacterial biofilms metabolic activity by a redox-reactive nanosensors array. J Nanobiotechnol 18:1–11. https://doi.org/10.1186/s12951-020-00637-y
48. Shiau AK, Massari ME, Ozbal CC (2008) Back to basics: label-free technologies for small molecule screening. Comb Chem High Throughput Screening 11:231–237. https://doi.org/10.2174/138620708783877807
49. Grieshaber D, MacKenzie R, Vörös J, Reimhult E (2008) Electrochemical biosensors-sensor principles and architectures Sensors 8:1400–1458. https://doi.org/10.3390/s80314000
50. Kellens E, Bové H, Vandenryt T, Lambrichts J, Dekens J, Drijkoningen S et al (2018) Micro-patterned molecularly imprinted polymer structures on functionalized diamond-coated substrates for testosterone detection. Biosens Bioelectron 118:58–65. https://doi.org/10.1016/j.bios.2018.07.032
51. Ogata AF, Edgar JM, Majumdar S, Briggs JS, Patterson SV, Tan MX et al (2017) Virus-enabled biosensor for human serum albumin. Anal Chem 89:1373–1381. https://doi.org/10.1021/acs.analchem.6b04840
52. Narang J, Malhotra N, Singhal C, Mathur A, Pundir C (2017) Detection of alprazolam with a lab on paper economical device integrated with urchin like Ag@ Pd shell nano-hybrids. Mater Sci Eng C 80:728–735. https://doi.org/10.1016/j.msec.2016.11.128
53. Ben-Yoav H, Dykstra PH, Bentley WE, Ghodssi R (2015) A controlled microfluidic electrochemical lab-on-a-chip for label-free diffusion-restricted DNA hybridization analysis. Biosens Bioelectron 64:579–585. https://doi.org/10.1016/j.bios.2014.09.069
54. Nwankire CE, Venkatanarayanan A, Glennon T, Keyes TE, Forster RJ, Ducree J (2015) Label-free impedance detection of cancer cells from whole blood on an integrated centrifugal microfluidic platform. Biosens Bioelectron 68:382–389. https://doi.org/10.1016/j.bios.2014.12.049
55. Channon RB, Yang Y, Feibelman KM, Geiss BJ, Dandy DS, Henry CS (2018) Development of an electrochemical paper-based analytical device for trace detection of virus particles. Anal Chem 90:7777–7783. https://doi.org/10.1021/acs.analchem.8b02042
56. Qi J, Li B, Zhou N, Wang X, Deng D, Luo L et al (2019) The strategy of antibody-free biomarker analysis by in-situ synthesized molecularly imprinted polymers on movable valve paper-based device. Biosens Bioelectron 142:111533. https://doi.org/10.1016/j.bios.2019.111533
57. Siavash Moakhar R, AbdelFatah T, Sanati A, Jalali M, Flynn SE, Mahshid SS et al (2020) A nanostructured gold/graphene microfluidic device for direct and plasmonic-assisted impedimetric detection of bacteria. ACS Appl Mater Interfaces 12:23298–23310. https://doi.org/10.1021/acsami.0c02654
58. Zhao H, Liu M, Jiang T, Xu J, Zhang H, Yu C et al (2020) Ultrasensitive monitoring of DNA damage associated with free radicals exposure using dynamic carbon nanotubes bridged interdigitated electrode array. Environ Int 139:105672. https://doi.org/10.1016/j.envint.2020.105672
59. Sanghavi BJ, Moore JA, Chávez JL, Hagen JA, Kelley-Loughnane N, Chou C-F et al (2016) Aptamer-functionalized nanoparticles for surface immobilization-free electrochemical detection of cortisol in a microfluidic device. Biosens Bioelectron 78:244–252. https://doi.org/10.1016/j.bios.2015.11.044
60. Wang Y, Xu H, Luo J, Liu J, Wang L, Fan Y et al (2016) A novel label-free microfluidic paper-based immunosensor for highly sensitive electrochemical detection of carcinoembryonic antigen. Biosens Bioelectron 83:319–326. https://doi.org/10.1016/j.bios.2016.04.062
61. Yukird J, Soum V, Kwon O-S, Shin K, Chailapakul O, Rodthongkum N (2020) 3D paper-based microfluidic device: a novel dual-detection platform of bisphenol A. Analyst 145:1491–1498. https://doi.org/10.1039/C9AN01738K
62. Hossain MM, Moon J-M, Gurudatt N, Park D-S, Choi CS, Shim Y-B (2019) Separation detection of hemoglobin and glycated hemoglobin fractions in blood using the electrochemical microfluidic channel with a conductive polymer composite sensor. Biosens Bioelectron 142:111515. https://doi.org/10.1016/j.bios.2019.111515
63. Sempionatto JR, Brazaca LC, García-Carmona L, Bolat G, Campbell AS, Martin A et al (2019) Eyeglasses-based tear biosensing system: non-invasive detection of alcohol, vitamins and glucose. Biosens Bioelectron 137:161–170. https://doi.org/10.1016/j.bios.2019.04.058
64. Boobphahom S, Ruecha N, Rodthongkum N, Chailapakul O, Remcho VT (2019) A copper oxide-ionic liquid/reduced graphene oxide composite sensor enabled by digital dispensing: non-enzymatic paper-based microfluidic determination of creatinine in human blood serum. Anal Chim Acta 1083:110–118. https://doi.org/10.1016/j.aca.2019.07.029
65. Bae CW, Toi PT, Kim BY, Lee WI, Lee HB, Hanif A et al (2019) Fully stretchable capillary microfluidics-integrated nanoporous gold electrochemical sensor for wearable continuous glucose monitoring. ACS Appl Mater Interfaces 11:14567–14575. https://doi.org/10.1021/acsami.9b00848
66. Singh R, Hong S, Jang J (2017) Label-free detection of influenza viruses using a reduced graphene oxide-based electrochemical immunosensor integrated with a microfluidic platform. Sci Rep 7:42771. https://doi.org/10.1038/srep42771
67. Chiu DT, deMello AJ, Di Carlo D, Doyle PS, Hansen C, Maceiczyk RM et al (2017) Small but perfectly formed? Successes, challenges, and opportunities for microfluidics in the chemical and biological sciences. Chem 2:201–223. https://doi.org/10.1016/j.chempr.2017.01.009
68. Narang J, Malhotra N, Singhal C, Mathur A, Pn AK, Pundir C (2017) Detection of alprazolam with a lab on paper economical device integrated with urchin like Ag@ Pd shell nano-hybrids. Mater Sci Eng C 80:728–735. https://doi.org/10.1016/j.msec.2016.11.128
69. Hong SA, Kim Y-J, Kim SJ, Yang S (2018) Electrochemical detection of methylated DNA on a microfluidic chip with nano-electrokinetic pre-concentration. Biosens Bioelectron 107:103–110. https://doi.org/10.1016/j.bios.2018.01.067
70. Parra-Cabrera C, Samitier J, Homs-Corbera A (2016) Multiple biomarkers biosensor with just-in-time functionalization: application to prostate cancer detection. Biosens Bioelectron 77:1192–1200. https://doi.org/10.1016/j.bios.2015.10.064

71. Chiriacò MS, Luvisi A, Primiceri E, Sabella E, De Bellis L, Maruccio G (2018) Development of a lab-on-a-chip method for rapid assay of Xylella fastidiosa subsp. pauca strain CoDiRO. Sci Rep 8:1–8. https://doi.org/10.1038/s41598-018-25747-4
72. Wang R, Xu Y, Sors T, Irudayaraj J, Ren W, Wang R (2018) Impedimetric detection of bacteria by using a microfluidic chip and silver nanoparticle based signal enhancement. Microchim Acta 185:184. https://doi.org/10.1007/s00604-017-2645-x
73. Siller IG, Preuss J-A, Urmann K, Hoffmann MR, Scheper T, Bahnemann J (2020) 3D-printed flow cells for aptamer-based impedimetric detection of E. coli crooks strain. Sensors 20:4421. https://doi.org/10.3390/s20164421
74. Ma W, Liu L, Xu Y, Wang L, Chen L, Yan S et al (2020) A highly efficient preconcentration route for rapid and sensitive detection of endotoxin based on an electrochemical biosensor. Analyst 145:4204–4211. https://doi.org/10.1039/D0AN00315H
75. Dos Santos MB, Queirós RB, Geraldes Á, Marques C, Vilas-Boas V, Dieguez L et al (2019) Portable sensing system based on electrochemical impedance spectroscopy for the simultaneous quantification of free and total microcystin-LR in freshwaters. Biosens Bioelectron 142:111550. https://doi.org/10.1016/j.bios.2019.111550
76. Núnez-Bajo E, Blanco-López MC, Costa-García A, Fernández-Abedul MT (2017) Integration of gold-sputtered electrofluidic paper on wire-included analytical platforms for glucose biosensing. Biosens Bioelectron 91:824–832. https://doi.org/10.1016/j.bios.2017.01.029
77. Narang J, Singhal C, Mathur A, Khanuja M, Varshney A, Garg K et al (2017) Lab on paper chip integrated with Si@ GNRs for electroanalysis of diazepam. Anal Chim Acta 980:50–57. https://doi.org/10.1016/j.aca.2017.05.006
78. Liu J, Zhang Y, Jiang M, Tian L, Sun S, Zhao N et al (2017) Electrochemical microfluidic chip based on molecular imprinting technique applied for therapeutic drug monitoring. Biosens Bioelectron 91:714–720. https://doi.org/10.1016/j.bios.2017.01.037
79. Park YM, Lim SY, Shin SJ, Kim CH, Jeong SW, Shin SY et al (2018) A film-based integrated chip for gene amplification and electrochemical detection of pathogens causing foodborne illnesses. Anal Chim Acta 1027:57–66. https://doi.org/10.1016/j.aca.2018.03.061
80. Safavieh M, Ahmed MU, Tolba M, Zourob M (2012) Microfluidic electrochemical assay for rapid detection and quantification of Escherichia coli. Biosens Bioelectron 31:523–528. https://doi.org/10.1016/j.bios.2011.11.032
81. Thiha A, Ibrahim F, Muniandy S, Dinshaw IJ, Teh SJ, Thong KL et al (2018) All-carbon suspended nanowire sensors as a rapid highly-sensitive label-free chemiresistive biosensing platform. Biosens Bioelectron 107:145–152. https://doi.org/10.1016/j.bios.2018.02.024
82. Laribi A, Allegra S, Souiri M, Mzoughi R, Othmane A, Girardot F (2020) Legionella pneumophila sg1-sensing signal enhancement using a novel electrochemical immunosensor in dynamic detection mode. Talanta 215:120904. https://doi.org/10.1016/j.talanta.2020.120904
83. Wang Y, Luo J, Liu J, Sun S, Xiong Y, Ma Y et al (2019) Label-free microfluidic paper-based electrochemical aptasensor for ultrasensitive and simultaneous multiplexed detection of cancer biomarkers. Biosens Bioelectron 136:84–90. https://doi.org/10.1016/j.bios.2019.04.032
84. Fan Y, Liu J, Wang Y, Luo J, Xu H, Xu S et al (2017) A wireless point-of-care testing system for the detection of neuron-specific enolase with microfluidic paper-based analytical devices. Biosens Bioelectron 95:60–66. https://doi.org/10.1016/j.bios.2017.04.003
85. Wei B, Mao K, Liu N, Zhang M, Yang Z (2018) Graphene nanocomposites modified electrochemical aptamer sensor for rapid and highly sensitive detection of prostate specific antigen. Biosens Bioelectron 121:41–46. https://doi.org/10.1016/j.bios.2018.08.067
86. Ming T, Wang Y, Luo J, Liu J, Sun S, Xing Y et al (2019) Folding paper-based aptasensor platform coated with novel nanoassemblies for instant and highly sensitive detection of 17β-estradiol. ACS Sens 4:3186–3194. https://doi.org/10.1021/acssensors.9b01633
87. Xie Y, Zhi X, Su H, Wang K, Yan Z, He N et al (2015) A novel electrochemical microfluidic chip combined with multiple biomarkers for early diagnosis of gastric cancer. Nanoscale Res Lett 10:477. https://doi.org/10.1186/s11671-015-1153-3
88. Garg M, Christensen MG, Iles A, Sharma AL, Singh S, Pamme N (2020) Microfluidic-based electrochemical immunosensing of ferritin. Biosensors 10:91. https://doi.org/10.3390/bios10080091
89. Moon J-M, Kim D-M, Kim MH, Han J-Y, Jung D-K, Shim Y-B (2017) A disposable amperometric dual-sensor for the detection of hemoglobin and glycated hemoglobin in a finger prick blood sample. Biosens Bioelectron 91:128–135. https://doi.org/10.1016/j.bios.2016.12.038
90. Ramalingam S, Chand R, Singh CB, Singh A (2019) Phosphorene-gold nanocomposite based microfluidic aptasensor for the detection of okadaic acid. Biosens Bioelectron 135:14–21. https://doi.org/10.1016/j.bios.2019.03.056
91. Lu L, Gunasekaran S (2019) Dual-channel ITO-microfluidic electrochemical immunosensor for simultaneous detection of two mycotoxins. Talanta 194:709–716. https://doi.org/10.1016/j.talanta.2018.10.091
92. Singh N, Ali MA, Rai P, Ghori I, Sharma A, Malhotra B et al (2020) Dual-modality microfluidic biosensor based on nanoengineered mesoporous graphene hydrogels. Lab Chip 20:760–777. https://doi.org/10.1039/C9LC00751B
93. Cincotto FH, Fava EL, Moraes FC, Fatibello-Filho O, Faria RC (2019) A new disposable microfluidic electrochemical paper-based device for the simultaneous determination of clinical biomarkers. Talanta 195:62–68. https://doi.org/10.1016/j.talanta.2018.11.022
94. Zhu L, Liu X, Yang J, He Y, Li Y (2020) Application of multiplex microfluidic electrochemical sensors in monitoring hematological tumor biomarkers. Anal Chem 92:11981–11986. https://doi.org/10.1021/acs.analchem.0c02430
95. Triroj N, Saensak R, Porntheeraphat S, Paosawatyanyong B, Amornkitbamrung V (2020) Diamond-like carbon thin film electrodes for microfluidic bioelectrochemical sensing platforms. Anal Chem 92:3650–3657. https://doi.org/10.1021/acs.analchem.9b04689
96. Fava EL, Silva TA, do Prado TM, de Moraes FC, Faria RC, Fatibello-Filho O. (2019) Electrochemical paper-based microfluidic device for high throughput multiplexed analysis. Talanta 203:280–286. https://doi.org/10.1016/j.talanta.2019.05.081
97. Alizadeh N, Salimi A, Sham T-K, Bazylewski P, Fanchini G (2020) Intrinsic enzyme-like activities of cerium oxide nanocomposite and its application for extracellular H2O2 detection using an electrochemical microfluidic device. ACS Omega 5:11883–11894. https://doi.org/10.1021/acsomega.9b03252
98. Martín A, Kim J, Kurniawan JF, Sempionatto JR, Moreto JR, Tang G et al (2017) Epidermal microfluidic electrochemical detection system: enhanced sweat sampling and metabolite detection. ACS Sens 2:1860–1868. https://doi.org/10.1021/acssensors.7b00729
99. Lee M-H, O'Hare D, Chen Y-L, Chang Y-C, Yang C-H, Liu B-D et al (2014) Molecularly imprinted electrochemical sensing of urinary melatonin in a microfluidic system. Biomicrofluidics 8:054115. https://doi.org/10.1063/1.4898152

100. Aymerich J, Márquez A, Terés L, Muñoz-Berbel X, Jiménez C, Domínguez C et al (2018) Cost-effective smartphone-based reconfigurable electrochemical instrument for alcohol determination in whole blood samples. Biosens Bioelectron 117:736–742. https://doi.org/10.1016/j.bios.2018.06.044
101. Lamas-Ardisana P, Martínez-Paredes G, Añorga L, Grande H (2018) Glucose biosensor based on disposable electrochemical paper-based transducers fully fabricated by screen-printing. Biosens Bioelectron 109:8–12. https://doi.org/10.1016/j.bios.2018.02.061
102. Gu S, Lu Y, Ding Y, Li L, Song H, Wang J et al (2014) A droplet-based microfluidic electrochemical sensor using platinum-black microelectrode and its application in high sensitive glucose sensing. Biosens Bioelectron 55:106–112. https://doi.org/10.1016/j.bios.2013.12.002

Publisher's note Springer Nature remains neutral with regard to jurisdictional claims in published maps and institutional affiliations.